RESEARCH REVIEW JOURNALS
Volume-03
Issue-11
November -2018

ISSN: 2455-3085 (Online)
RESEARCH REVIEW International Journal of Multidisciplinary
www.rrjournals.com [UGC Listed Journal]

Synthesis, Characterization and Photocatalytic Properties of Iron Oxide Nanoparticles Synthesized by Sol-Gel Autocombustion with Ultrasonic Irradiation

Anurag Gan

Department of Chemistry, Centurian University, Bhubaneswar (India)

ARTICLE DETAILS

Article History
Published Online: 10 November 2018

Keywords
Fe2O3; Sol–Gel; Auto-combustion; Ultrasonic irradiation; Optical properties; Reactive Red 4

ABSTRACT

Iron oxide (Fe_2O_3) nanoparticles were prepared by combination of sol-gel auto-combustion and ultrasonic irradiation. The XRD pattern reveals that the crystallite size of sample is 36.7 nm and the phase identification shows hematite, syn has been crystalized. The morphology of the sample investigated by FESEM showed that particle size of the sample was about 76 nm. The optical property of Fe_2O_3investigated by DRS showed that there may exist three energy band gaps in iron oxide nanoparticles. FT-IR technique was used to determine the functional group of product. In agreement to XRD results, the result of FT-IR revealed no organic residue in product. Photo catalyst nanoparticles were immobilized on the surface of glass slide using Doctor Blade method. Photocatalytic degradation of reactive red 4 (RR4) was investigated under UV light using iron oxide nanoparticles as catalyst. The kinetic of RR4 degradation under UV light irradiation in the presence of Fe_2O_3 as photocatalyst, and rate constant was determined. Experiments exhibited that Fe_2O_3 nanoparticles decomposed 52% of azo dye RR4 in solution duration 135 min. The photo catalytic reaction kinetic of RR4 degradation in the presence of Fe_2O_3 nanoparticles followed Langmuir-Hinshelwood model with the rate constant of about 0.005 min^{-1}.

1. Introduction

Dyes are an important class of chemicals which are widely used in several industrial processes such as leather, textile and printing industries. The release of the dyes in the effluents of these industries may cause major environmental problems. Most of these dyes are hazardous material because they can cause cancer, genetic mutation or other effects[1]. Various treatment processes and techniques have been used to remove the dye pollutants from contaminated water[2-5]. Photocatalytic degradation of organic pollutants over semiconductors has been extensively studied for more than 30 years[6]. Heterogenous photocatalysis is one the most successful methods for removal of dye pollutants in wastewater[7]. Hematite (α-Fe_2O_3), as an n-type semiconductor (Eg=1.8-2.2) and the most thermodynamically stable species of iron oxides, has been widely applied and studied in recent years[8-10]. Wang has evaluated pure and gold-deposited iron oxide aerogels for the photocatalytic degradation of disperse blue 79 dye in water, which is an azo dyestuff popularly seen in the textile wastewater. Sajjadi and Goharshadi have fabricated highly monodispersed crystalline hematite with similar cube shape via ultrasound assisted hydrothermal techniques which was used for photo degradation of three organic dyes, ractive black 5(Rb5), methylene blue(MB) and rhodamine B (RhB). Poros hematite has been applied for treatment As(v) from aqeous solution as adsorbant. Hematit is nontoxic, cheap and good resistant to corrosion. Various methods can be used for the preparation of α-Fe_2O_3 with high crystallinity. α-Fe_2O_3 nanoparticles are immoblized on different substrates. Li and coworkers have prepared a series of Fe_2O_3/Al_2O_3 samples by sol-gel method using ferric nitrate, aluminium nitrate and glycol as starting material. Xu and coworker reported alumina-dispersed α-Fe_2O_3 (Fe_2O_3/alumina) which is not more photoactive than the unsupported α-Fe_2O_3.

In this work, α-Fe_2O_3 nanoparticles are synthesized with sol gal autocombustion method in combination with ultrasonic irradiation. This technique is convenient and cheap. A paste of α-Fe_2O_3 nanoparticls with terpinol and ethyl celloluse is prepared and a glass slide is coated with this paste. In this condition, photocatalyst nanoparticles are immobilized on glass slide as heterogenous photocatalyst providing the possibility of easy and fast reuse of catalyst. Photocatalytic degradation of Reactive Red 4 in oxygenated solution is used to determine the photocatalytic activity. Finally, the kinetic order and constant rate of RR4 degradation are determined.

2. Experimental

- ***Materials***

The precursor material, iron (III) nitrate nonahydrate, $Fe(NO_3)_3.9H_2O$ was obtained from Merck Chemical company. Ethyl alcohol and glycine were supplied by Sigma-Aldrich Chemical Co. Distilled water was used throughout.

- ***Synthesis of iron oxide nanoparticles***

Iron oxide powders were synthesized from sol-gel auto combustion by ultrasonic irradiation method. 0.01 mol of $Fe(NO_3)_3.9H_2O$ (4.102 g) was dissolved in 20 ml distilled water by stirring on hotplate at 90^oC. Then, 0.0025 mol glycine ($C_2H_5NO_2$) 0.190 g was added to solution to chelate metal ion. An ammonia solution (21%) was added to adjust the pH value to 9.5. The clear solution was refluxed 2h at 100^oC to get complex in N_2 atmosphere. Then, solution was placed in ultrasonic irradiation bath at 40^oC for 45 minutes. This solution was heated at 175^oC until solutions were evaporated slowly and the viscous gels were formed. Gel was transferred to cruse and heated at 90^oC for 13h. Then, product was calcined at 675^0C for 4h.

• ***Coating on glass using nanoparticles pastes by Doctor Blade method***

To stabilize iron oxide nanaoparticles on substrate, first, we prepared a paste of iron oxide nanoparticles by adding terpinol, ethyl ethyl cellulose**,** acetic acid, ethnol and double distilled water under certain process that showed in flow chart (Fig. 1). Then, paste was used for coating on glass by Doctor Blade method, the area of the photo catalyst coated on glass was 11cm^2.The photo catalyst coated glass was air dried, and sintering at 300^{o}C in air to remove residual solvent and any organic compounds to improve the contact between the film and the substrate.

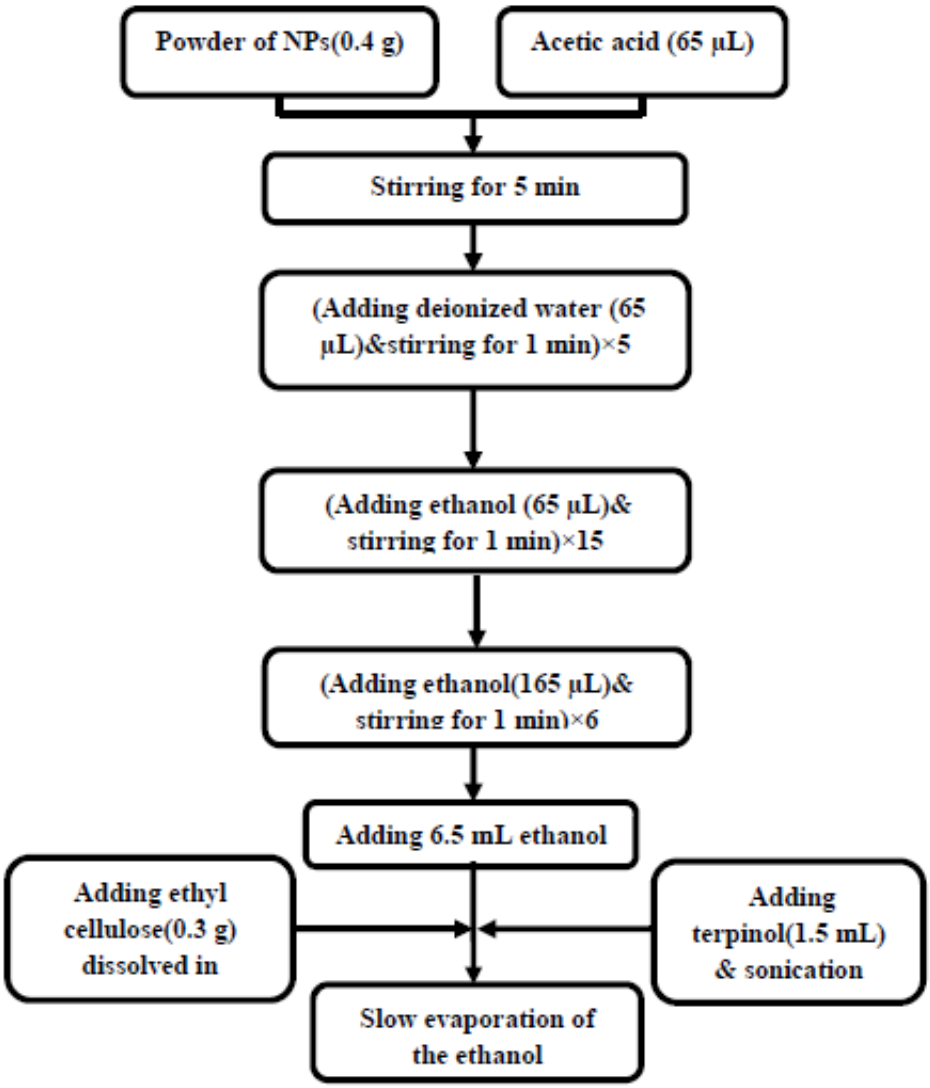

Fig.1. Flow chart for preparation of iron oxide nanoparticles paste.

• ***Characterization***

FT-IR absorption spectrum of sample after calcination was obtained using KBr disks on a FT-IR 6300. Powder X-ray diffraction analysis was performed on a D8 Advance, BRUKER diffractometer in the diffraction angle range 2θ=5-80° with Cu Kα radiation (1.5406 A°). Diffuse reflectance spectra (DRS) were collected with a V-670, JASCO spectrophotometer and transformed to the absorption spectra according to the Tauc relationship. Field emission scanning electron microscopy (FESEM) images was taken on a Hitachi, S-4160 scanning electron microscope. The concentration of azo dyes solutions was determined using its absorbance by a Cary 500 UV–Vis spectrophotometer.

3. Results and Discussions

• ***XRD analysis***

X-ray diffraction was used to characterize the phase and crystal property of calcined iron oxide nanoparticles synthesized by sol-gel auto combustion with ultrasonic irradiation. The diffraction peaks of the sample (Fig. 2) match well with the standard pattern of Rhombohedral hematite, syn (JCPDS card no. 33.0664), where the diffraction peaks at 2θ values of 27.77, 38.4, 41.5, 47.7, 57.9, 63.5, 73.8 and 75.7 can be ascribed to the reflections of (012), (104), (110), (113), (024), (116), (214) and (300), respectively. No peaks for any impurities are observed, indicating high purity of the product. The average crystallite size of Fe_2O_3calculated from X-ray line

broadening using Scherrer's equation was found to be about 36.7 nm.

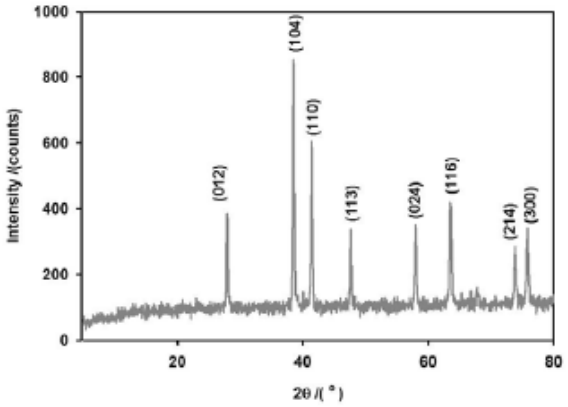

Fig.2. XRD pattern of iron oxide nanoparticles prepared by sol-gel auto-combustion with ultrasonic irradiation.

- ***FESEM characterization***

The morphology of the sample was investigated by FESEM. Fig. 3 indicates that the sample prepared by sol-gel autocombustion with ultrasonic irradiation consists of spherical particles and the effect of sintering is observed. It clearly shows that the diameter of particles is 76 nm.

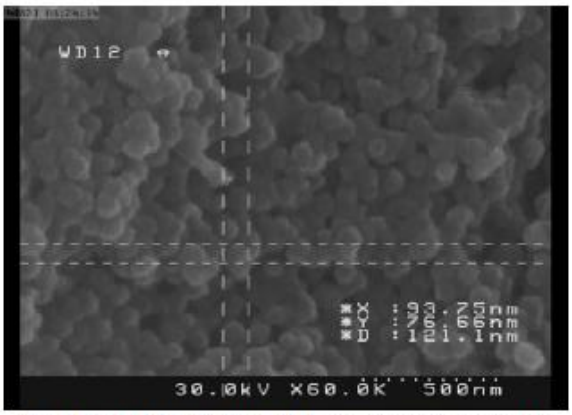

Fig.3. FESEM image of iron oxide nanoparticles prepared by sol-gel auto-combustion with ultrasonic irradiation.

- ***FTIR analysis***

The FTIR spectrum was used to identify the functional groups on the surface of the Fe_2O_3. Fig. 4 represents the IR spectrum of sample after calcination. The peak at 3440 cm^{-1}arises from stretching vibration of O−H and the peak located at around 1624 cm^{-1}can be ascribed to bending vibrations of adsorbed water molecules on surface of nanoparticles. The weak band at 1127cm^{-1}can be assigned to residue FeOOH in structure. The observed peak at 914cm^{-1} can be related to stretching vibration of C−O group. The peaks at 544 and 477.4 cm^{-1}arises from Fe−O−Fe vibrations.

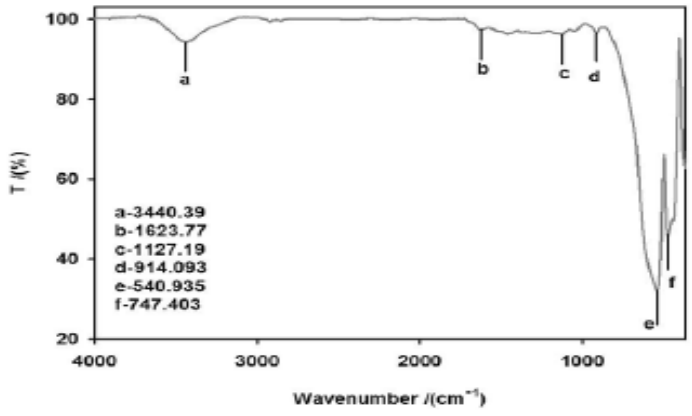

Fig.4. FT-IR spectrum of iron oxide nanoparticles prepared by sol-gel auto-combustion with ultrasonic irradiation after calcination.

• ***DRS analysis***

UV–Vis diffuse reflectance spectra of Fe_2O_3 prepared by sol-gel autocombustion with ultrasonic irradiation were collected. It can be clearly seen from Fig. 5 that absorbance of Fe_2O_3 is in the range of 200–850 nm indicating that the band edge absorption has been broadened to visible light region. UV–Vis absorption spectroscopy method has been extensively applied to investigate the optical properties of various kinds of optoelectronic. UV–Vis spectrum of $Fe_2O_3$was taken as a function of wavelength. The optical band gap of Fe_2O_3 was calculated using Tauc relation $\alpha h\nu = A (h\nu - Eg)^n$, where α is the absorption coefficient, A is a constant and n is an index with the values 1/2, 3/2,2 and 3, depending on the nature of electronic transition, where n=1/2 for direct band gap semiconductors. An extrapolation of the linear region of plot $(\alpha h\nu)^2$vs hν gives the value of the optical band gap Eg as shown in Fig.6.The measured band gap of iron oxide was found to be 2.11 eV.

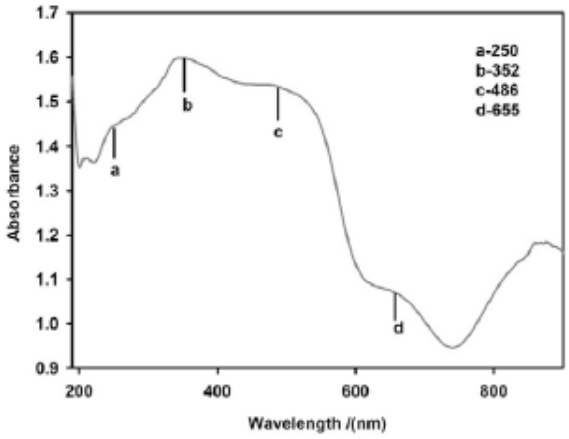

Fig. 5. UV–Vis absorption spectrum of iron oxide nanoparticles prepared by combination sol-gel auto-combustion with ultrasonic irradiation.

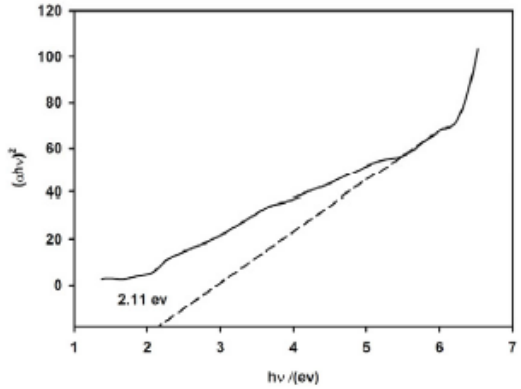

Fig.6.Tauc plot of iron oxide nanoparticles prepared by combination sol-gel auto-combustion with ultrasonic irradiation.

• ***Photocatalytic studies of Fe_2O_3***

Photocatalytic activity of Fe_2O_3 was investigated through Reactive Red 4 (RR4) degradation under UV-light irradiation. Fig. 7 shows the chemical structure of RR4. For immobilization Fe_2O_3 nanoparticles, the paste of Fe_2O_3 prepared and then a thin layer of paste was coated on glass slide with doctor Blade method as mentioned in section 2.3. To determine dye degradation percentage by photo catalyst, first standard solutions with different concentrations of RR4 were prepared and their UV-Vis spectra were recorded (inserted in Fig. 8). Then, the graph of absorbance in maximum wavelength (λ_{max}=534 nm) vs concentration was plotted and the equation of the most fitted line was obtained (Fig.8). This equation was used to determine the concentration of RR4. In the following a RR4 solution with a concentration of 10.4 ppm was exposed at O_2 gas for 30 min. The immobilized photocatalyst was placed in a petri dish contained 25 of above dye solution. The mixture of RR4 and immobilized photocatalyst was stirred in the dark condition to allow the mixture to establish sorption and desorption equilibrium of dye molecules by the photo catalyst nanoparticles. The UV-Vis absorbance spectrum of RR4 solution after dark condition showed a minor change. Then, petri dish was exposed under UV light irradiation for a certain time and after each time UV-Vis spectrum was recorded. The degradation process continued till 135 min UV light irradiation. Fig. 9 shows absorption spectra of RR4 degradation using iron oxide nanoparticles prepared by sol-gel autocombustion with ultrasonic irradiation under different irradiation time. Degradation rate was calculated using the following equation:

$$\text{Degradation rate (\%)} = \left[\frac{c_0 - c_t}{C}\right] \times 100$$

where C_o is the initial concentration of dye and C_t is the concentration of pollutant at time t.

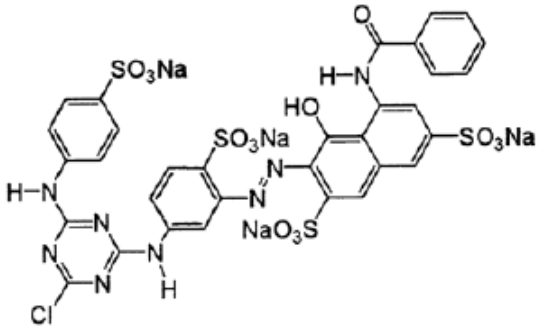

Fig. 7. Chemical structure of Reactive Red 4.

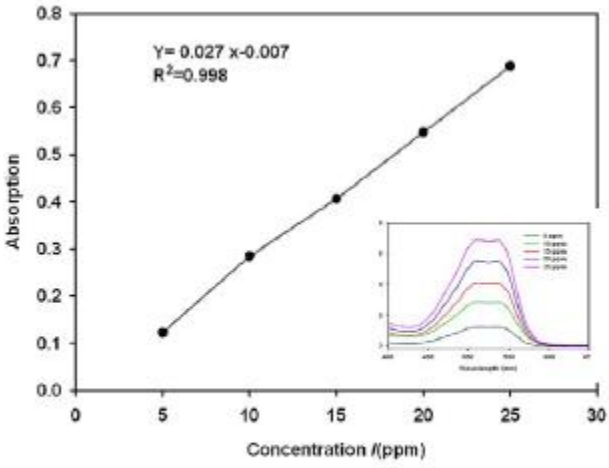

Fig. 8. Calibration curve of Reactive Red 4 and absorption spectra of Reactive Red 4 in defined concentrations.

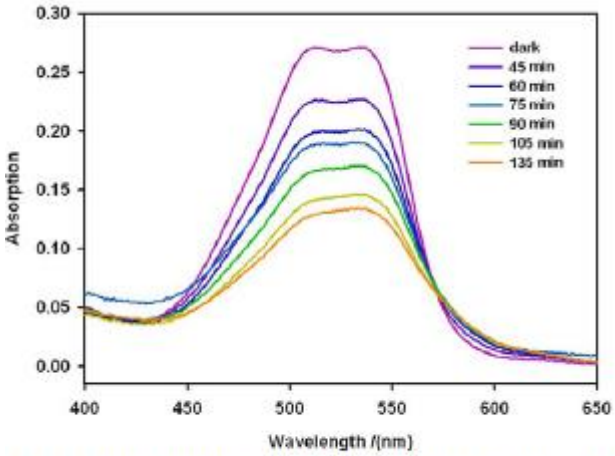

Fig. 9. Absorption spectra of the Reactive Red 4 solution with initial concentration of 10.3 mg/L under UV irradiation and using iron oxide as photocatalyst.

The degradation percentage of RR4 in the presence of Fe_2O_3 photocatalystis was about 52% (Fig. 10). Photocatalytic reaction kinetic can be expressed by the Langmuir–Hinshelwood(L–H) model,

$$\ln(C_t/C_0)=K_{app}t$$

where k_{app} is the apparent pseudo first order reaction rate constant and t is the reaction time. A plot of $\ln(C/C_o)$ vs t will yield a slope of k_{app}. The rate constant of degradation of RR4 in the presence of Fe_2O_3 under UV light irradiation equals to 0.005 min^{-1} (Fig.11).

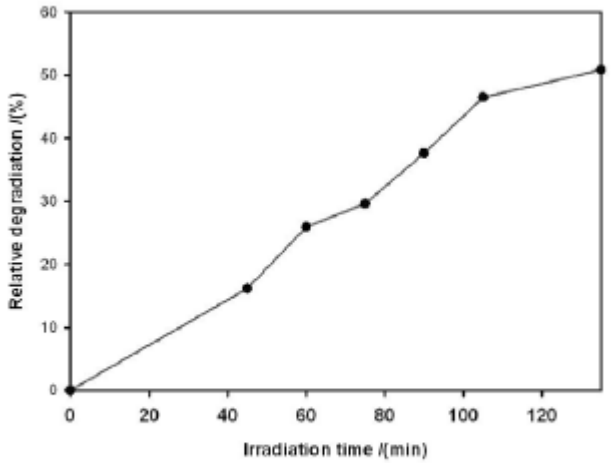

Fig. 10. Relative degradation of RR4 in the presence of iron oxide nanoparticles under UV light irradiation.

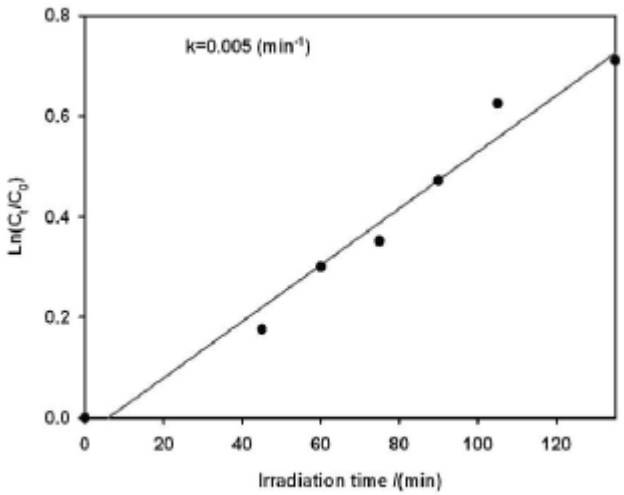

Fig. 11. The kinetic plot of photocatalytic degradation of RR4

- ***Mechanism of photocatalytic degradation***

In the presence of UV light irradiation, an electron in Fe_2O_3 is excited, producing conduction band electron (e^-_{CB}) and valence band holes (h^+). The photogenerated holes at the surface of Fe_2O_3 can react with H_2O to produce $OH^·$ radicals, which are strong oxidants capable of oxidizing many organic pollutants, resulting in degradation of pollutants. The photogenerated electron can either recombine with the positive holes or react with available O_2 to produce super oxide ions (O_2^-) that subsequently produce hydroproxyl radicals which in turn may react further to form H_2O_2 and more $OH^·$ radicals.

4. Conclusion

α-Fe_2O_3 nanoparticles were successfully synthesized using sol-gel autocombustion method with ultrasonic irradiation. The property of sample was characterized by XRD, FESEM, FTIR and DRS. α- Fe_2O_3 NP coated on glass successfully degraded 52% oxygenated RR4 solution in 135 min under UV light irradiation.The RR4 degradation kinetic in the presence of α- Fe_2O_3 NP stabilized on glass followed Langmuir-Hinshelwood model and pseudo first order rate constant was about 0.005 min^{-1}.

References

1. Hayat K, Gondal MA, Khaled MM, Yamani ZH, Ahmed S. Laser induced photocatalytic degradation of hazardous dye (Safranin-O) using self synthesized nanocrystalline WO3. Journal of Hazardous Materials. 2011;186(2-3):1226-33.
2. Wu J, Wang J, Li H, Du Y, Huang K, Liu B. Designed synthesis of hematite-based nanosorbents for dye removal. Journal of Materials Chemistry A. 2013;1(34):9837.
3. Samiee S, Goharshadi EK. Graphene nanosheets as efficient adsorbent for an azo dye removal: kinetic and thermodynamic studies. Journal of Nanoparticle Research. 2014;16(8).
4. Lu Y-S, Bastakoti BP, Pramanik M, Malgras V, Yamauchi Y, Kuo S-W. Direct Assembly of Mesoporous Silica Functionalized with Polypeptides for Efficient Dye Adsorption. Chemistry - A European Journal. 2015;22(3):1159-64.
5. Barreto-Rodrigues M, Silveira J, Zazo JA, Rodriguez JJ. Synthesis, characterization and application of nanoscale zero-valent iron in the degradation of the azo dye Disperse Red 1. Journal of Environmental Chemical Engineering. 2017;5(1):628-34.

6. Ollis DF, Al-Ekabi H. Photocatalytic purification and treatment of water and air: proceedings of the 1st International Conference on TiO2 Photocatalytic Purification and Treatment of Water and Air, London, Ontario, Canada, 8-13 November, 1992: Elsevier Science Ltd; 1993.
7. Hoffmann MR, Martin ST, Choi W, Bahnemann DW. Environmental Applications of Semiconductor Photocatalysis. Chemical Reviews. 1995;95(1):69-96.
8. Ahmad R, Ahmad Z, Khan AU, Mastoi NR, Aslam M, Kim J. Photocatalytic systems as an advanced environmental remediation: Recent developments, limitations and new avenues for applications. Journal of Environmental Chemical Engineering. 2016;4(4):4143-64.
9. Von Rudorff GF, Jakobsen R, Rosso KM, Blumberger J. Fast Interconversion of Hydrogen Bonding at the Hematite (001)–Liquid Water Interface. The Journal of Physical Chemistry Letters. 2016;7(7):1155-60.
10. Hao H, Sun D, Xu Y, Liu P, Zhang G, Sun Y, et al. Hematite nanoplates: Controllable synthesis, gas sensing, photocatalytic and magnetic properties. Journal of Colloid and Interface Science. 2016;462:315-24.

